

# Optimized Transcutaneous Spinal Cord Direct Current Stimulation using Multiple Electrodes from 3/9/7 System\*

Yu Huang<sup>1,2</sup>, Chris Thomas<sup>1</sup>, Abhishek Datta<sup>1</sup>

**Abstract**— Transcutaneous spinal cord direct current stimulation (tSDCS) has been applied as an easy non-invasive approach to modulate spinal cord functions. Currently there is no formal layout or guidelines for electrode placement to optimize tSDCS. Most clinical applications simply place the stimulating electrode over the intended spinal cord target. Here we show that this *ad hoc* method cannot achieve optimal stimulation. Specifically, we propose a new electrode layout for optimized tSDCS. The candidate high-definition electrodes distribute on the back of the body evenly and the layout was named 3/9/7 system. Algorithmic optimization was performed leveraging this electrode placement system and a 1 mm<sup>3</sup> human full body model. Results show that the optimal stimulation montages cannot be trivially determined and they outperform the unoptimized stimulation configuration. This work opens the possibility for systematic treatment planning in future clinical applications of tSDCS.

## I. INTRODUCTION

Transcutaneous spinal cord direct current stimulation (tSDCS) is a technique similar to transcranial direct current stimulation (tDCS) that delivers weak direct current (up to 2 mA) to the spinal cord thereby providing similar advantages: cheap, portable, ease of use, and non-invasive with common adverse events restricted to skin itching [1]. The potential to modulate spinal cord function opens the possibility to explore not only physiological effects but also clinical applications for numerous disorders linked to spinal cord dysfunction such as amyotrophic lateral sclerosis (ALS), spinal cord injury (SCI), etc. Studies to-date have indicated promising results such as improving motor unit recruitment and shortening peripheral silent period [2],

As with any electrical stimulation modality, the pivotal factor for tSDCS efficacy and safety is the spatial extent of the induced electric field/current density. Electrode placement for tSDCS is currently planned by placing an electrode over the intended spinal cord target region to be modulated with the return electrode placed in a functionally unrelated area. Computational modeling studies indicate that employing the aforementioned bipolar scheme results in maximum electric field not directly underneath but between the electrodes [3]. This therefore implies that tSDCS studies conducted to-date did not deliver the maximum or optimal electric field to the intended target. Nonetheless there continues to be

ample evidence that tSDCS modulates spinal cord function. However, the development of a true clinical utility requires establishing robust and prolonged effects. Since it is rational to assume that regions subject to maximal electric field will elicit maximal modulation based on *in vitro* model [4], stimulation strategies that will ensure maximal electric field at the target of choice is of immense interest.

In this study, we propose a novel, multi-electrode paradigm (similar to the approach employed on the cranium successfully over the past decade [3], [5]) in targeting the spinal cord. The advantage of using multiple small electrodes are manifold: from reducing skin sensation to ability to leverage optimization tools. The methods of our optimization procedure are based on the one employed on the head previously [5]. Specifically, precise forward models of tSDCS current flow for all possible sets of electrode pairs are first computed. This results in a linear system relating skin current distribution to the electric field. Since the fields generated by each electrode pair superpose in a linear fashion, linear algebraic operations may be utilized to obtain optimal parameters (electrode placement, individual electrode current to be injected, etc.) These parameters are restricted by user-defined criterion such as intensity or focality at target, field direction, maximum total current reflecting safety limit, etc.

Since there is no known electrode placement scheme for the spinal cord, we introduce one based on the classical 10/10 approach. Specifically, we propose a electrode placement layout which we named “3/9/7” system. Each of the electrodes serve as candidates for injecting current based on the user-chosen criterion. We compared the achieved electric field intensity at interested region in the spinal cord from optimized stimulation to an *ad hoc* 4×1 montage [3], and found that optimization does increase the field intensity at the target.

## II. METHODS

A high resolution (1 mm<sup>3</sup>), anatomically accurate human body model was obtained from the ITIS Virtual Population [6]. Simpleware ScanIP (Simpleware Ltd, Exeter, UK) was used to combine and simplify the original 22 tissue segmentations into these masks: brain gray matter, brain white matter, cerebrospinal fluid (CSF), gastrointestinal system, liver, kidney, bladder, reproductive system, respiratory system, bone, cartilage, muscle, and skin. The spinal cord in the model was further manually segmented into spinal white matter and spinal gray matter. Spinal nerves were also segmented manually using Pocket Anatomy Volume 3 [7]

\*This work was supported by the NIH through grant 5R44NS092144-04

<sup>1</sup>Y. Huang, C. Thomas and A. Datta are with Research & Development, Soterix Medical, Inc., New York, NY 10001, USA yhuang at soterixmedical.com

<sup>2</sup>Y. Huang is with the Department of Biomedical Engineering, City College of the City University of New York, New York, NY 10031, USA yhuang16 at citymail.cuny.edu

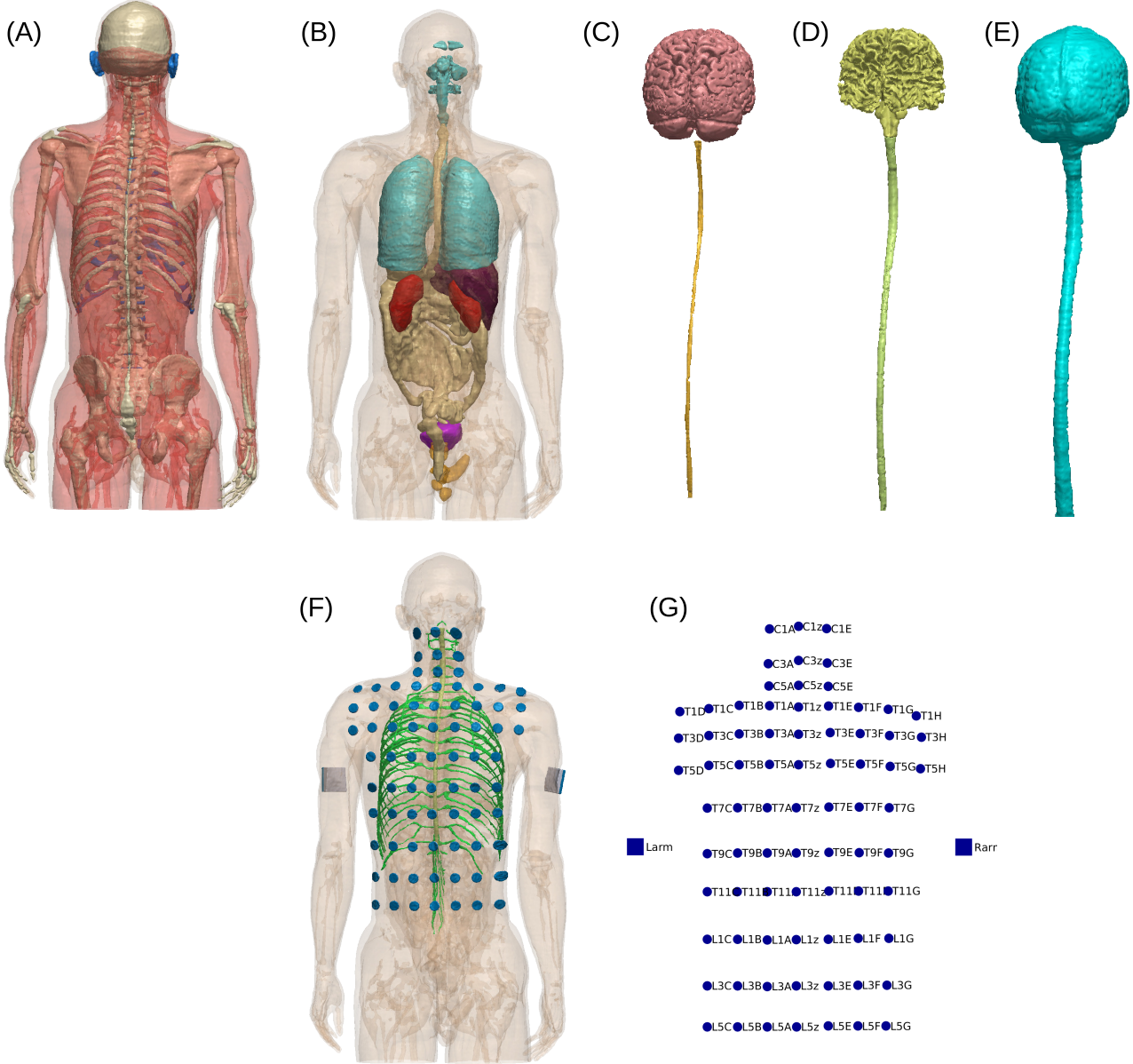


Fig. 1. Visualization of the model used for optimization of tSDCS. (A) bone, cartilage, muscle, and skin; (B) viscera including respiratory system, gastrointestinal system, liver, kidney, bladder, and the reproductive system; (C) cerebrospinal fluid (CSF); (D) brain and spinal gray matter; (E) brain and spinal white matter; (F) spinal nerves, with electrodes placed; (G) electrode layout with names.

and Bio Digital [8] as the reference. In total 16 different tissues were included in the model, see Figure 1.

Electrodes and gel were modeled as 20 mm diameter disks and positioned in ScanIP over the spine, to be roughly over the vertebrae (the Cervical 1-5, Thoracic 1-12, and Lumbar 1-5 spinal vertebrae). Each electrode along the spine was named with the corresponding vertebrae and an additional suffix “z”, except C6-C7 due to limited space anatomically. Additional electrodes placed to the left or right of the center electrodes have the same vertebrae prefix, with a suffix of either a letter from “A” to “D” if placed on the left, or a letter from “E” to “H” if placed on the right. The layout is

shown in Figure 1 (Panels FG). Since there are 3 columns of electrodes in the cervical area of the spine, 9 columns in the thoracic area, and 7 columns in the lumbar region, we named this electrode layout as 3/9/7 system.

Volume conductor modeling follows the same procedures as the tDCS modeling (see [9] for details). Specifically, all the geometry in the model was meshed in ScanIP. Electric field distribution was solved for all the bipolar electrode configurations (with C1z as the reference). This was done in Abaqus (SIMULIA, Providence, RI) for 1 A/m<sup>2</sup> current density injected at the anode and ground for the cathode. Literature tissue conductivities were

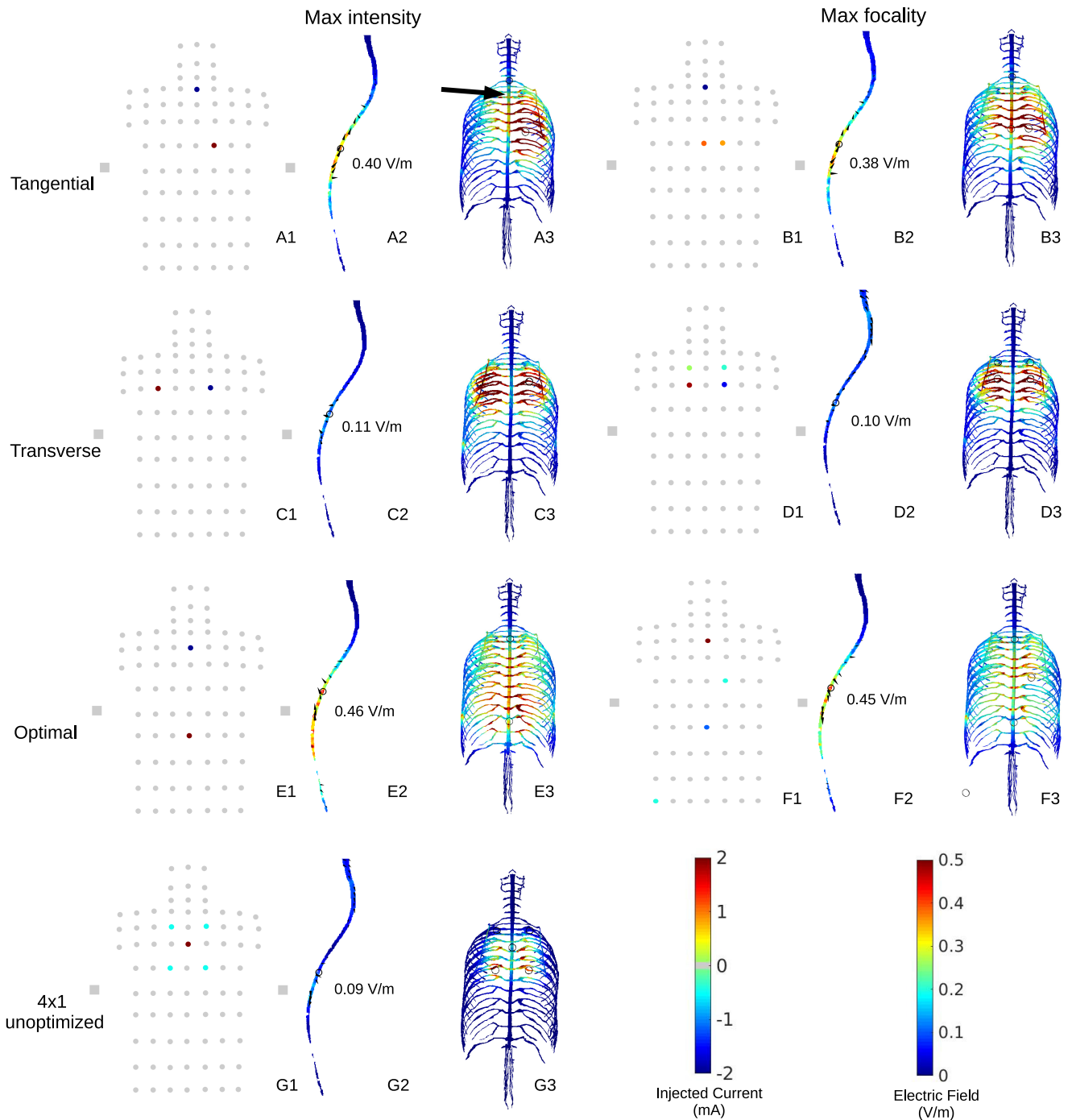


Fig. 2. Results of optimized spinal cord stimulation targeting T5. The three subplots (labeled by numbers) at each panel (labeled by letters) show the optimal electrode montage (with injected current intensities color coded; gray is candidate electrodes), the distribution and direction of the optimal electric field in one sagittal slice of the spinal cord, and a 3D rendering of the electric field magnitude in the spinal cord and nerves (dorsal view). Max-intensity and max-focality are shown in Panels ACE and BDF, respectively, with the electric field optimized along tangential (Panels AB), transverse (Panels CD), as well as the optimal direction where the electric field magnitude is maximized (Panels EF). We also show the unoptimized case in Panel G. Target location is indicated by the black circles in the sagittal slices and also an arrow in Panel A3. Field intensity at the target is noted. Electrode locations are also shown as black circles in the 3D renderings.

assigned [6], [10] (in S/m): electrode- $5.9 \times 10^7$ , gel-0.3, brain and spinal gray matter-0.276, brain and spinal white matter-0.126, spinal nerves-0.126, CSF-1.65, gastrointestinal system-0.164, liver-0.221, kidney-0.403, bladder-0.408, reproductive system-0.232, respiratory system- $10^{-7}$ , bone-0.01, cartilage-1.01, muscle-0.35, skin-0.465. All the solutions were then calibrated to correspond to 1 mA stimulation.

We applied the same mathematical framework as in [5] to optimize stimulation of the spinal cord. We aim to target the spinal cord at a representative thoracic location of T5. We attempted to optimize the stimulation according to two criteria: (1) maximize the electric field intensity at the target without considering how focal the stimulation is (max-intensity); (2) make the stimulation as focal as possible at the target but ignoring its intensity (max-focality). Specifically, (1) is done by linear programming, and (2) is implemented by least square, with field strength properly weighted at target and non-target regions (see [5] for details). The total injected current was constrained as 2 mA. Each criterion was run for three different directions of the electric field at the target: tangential (current flow at the direction tangential to the local curvature of the spinal cord); transverse (current flow from left to right); and optimal (the best direction where the magnitude of the electric field is maximized, see [11]).

### III. RESULTS

Figure 2 shows the electric field distributions and the optimal electrode montages for the optimization results under different user-controlled criteria, and the *ad hoc*  $4 \times 1$  configuration. The optimal montages are as follows: (1) for max-intensity: tangential direction – T7E (2 mA), T1z (-2 mA); transverse direction – T5B (2 mA), T5E (-2 mA); optimal direction – T11z (2 mA), T3z (-2 mA); (2) for max-focality: tangential direction – T7z (1.12 mA), T7E (0.88 mA), T1z (-2.00 mA); transverse direction – T5A (1.89 mA), T5E (-1.64 mA), T3A (0.11 mA), T3E (-0.36 mA); optimal direction – L5C (-0.39 mA), T11z (-1.17 mA), T7E (-0.44 mA), T3z (2.00 mA). It is obvious that optimized stimulation gives higher electric field at the target than the unoptimized  $4 \times 1$  montage. We also note that max-intensity criterion can always achieve higher field intensity compared to max-focality stimulation, with a small loss in focality. It seems that it is easier to get higher stimulation strength if the current flows along the spinal cord rather than transverse (comparing Tangential vs Transverse), but the best direction of current flow is not exactly tangential to the spinal cord (see Optimal). The corresponding electrode montage indicates that this cannot be trivially determined, and one needs to turn to algorithmic approach which is presented here.

### IV. DISCUSSION

This work proposes a novel electrode placement layout for optimized transcutaneous spinal cord direct current stimulation using high-definition electrodes. The proposed system (“3/9/7”) follows similar definition of the 10/10 layout. Mathematical optimization on a single target in the spinal cord showed that optimal stimulation elicits higher

and more focal electric field at the target compared to *ad hoc*, unoptimized case (e.g.,  $4 \times 1$  montage). These results show that the best stimulation montage cannot be trivially determined manually. Note all these results are based on the assumption that higher and focal electric field elicits higher modulation [4].

Future work will explore the optimized stimulation also in the cervical and lumbar regions of the spinal cord. Optimization for stimulation of multiple locations in the spinal cord can also be studied following the work in [12]. The approach proposed here can also be applied to stimulate targeted locations on the spinal nerves. The predictions made in this study regarding optimized electrode configurations should also be experimentally verified in the future.

### REFERENCES

- [1] F. Cogiamanian, G. Ardolino, M. Vergari, R. Ferrucci, M. Ciocca, E. Scelzo, S. Barbieri, and A. Priori, “Transcutaneous Spinal Direct Current Stimulation,” *Frontiers in Psychiatry*, vol. 3, Jul. 2012. [Online]. Available: <https://www.ncbi.nlm.nih.gov/pmc/articles/PMC3389353/>
- [2] T. Bocci, B. Vannini, A. Torzini, A. Mazzatorta, M. Vergari, F. Cogiamanian, A. Priori, and F. Sartucci, “Cathodal transcutaneous spinal direct current stimulation (tsDCS) improves motor unit recruitment in healthy subjects,” *Neuroscience Letters*, vol. 578, pp. 75–79, Aug. 2014.
- [3] A. Datta, V. Bansal, J. Diaz, J. Patel, D. Reato, and M. Bikson, “Gyri-precise head model of transcranial DC stimulation: Improved spatial focality using a ring electrode versus conventional rectangular pad,” *Brain stimulation*, vol. 2, no. 4, pp. 201–207, Oct. 2009.
- [4] M. Bikson, M. Inoue, H. Akiyama, J. K. Deans, J. E. Fox, H. Miyakawa, and J. G. R. Jefferys, “Effects of uniform extracellular DC electric fields on excitability in rat hippocampal slices *in vitro*,” *The Journal of Physiology*, vol. 557, no. 1, pp. 175–190, 2004.
- [5] J. P. Dmochowski, A. Datta, M. Bikson, Y. Su, and L. C. Parra, “Optimized multi-electrode stimulation increases focality and intensity at target,” *Journal of Neural Engineering*, vol. 8, no. 4, p. 046011, Aug. 2011.
- [6] A. Christ, W. Kainz, E. G. Hahn, K. Honegger, M. Zeffner, E. Neufeld, W. Rascher, R. Janka, W. Bautz, J. Chen, B. Kiefer, P. Schmitt, H.-P. Hollenbach, J. Shen, M. Oberle, D. Szczesba, A. Kam, J. W. Guag, and N. Kuster, “The Virtual Family—development of surface-based anatomical models of two adults and two children for dosimetric simulations,” *Physics in Medicine and Biology*, vol. 55, no. 2, pp. N23–N38, Jan. 2010.
- [7] T. B. Müller and E. Reif, *Pocket Atlas of Sectional Anatomy, Volume III: Spine, Extremities, Joints: Computed Tomography and Magnetic Resonance Imaging*, 2nd ed. Stuttgart ; New York: Thieme, Dec. 2016.
- [8] J. Qualter, F. Sculli, A. Oliker, Z. Napier, S. Lee, J. Garcia, S. Frenkel, V. Harnik, and M. Triola, “The biodigital human: a web-based 3d platform for medical visualization and education.” *Studies in health technology and informatics*, vol. 173, pp. 359–361, 2012. [Online]. Available: <http://europepmc.org/abstract/med/22357018>
- [9] Y. Huang, J. P. Dmochowski, Y. Su, A. Datta, C. Rorden, and L. C. Parra, “Automated MRI segmentation for individualized modeling of current flow in the human head,” *Journal of Neural Engineering*, vol. 10, no. 6, p. 066004, Dec. 2013.
- [10] Y. Huang, A. A. Liu, B. Lafon, D. Friedman, M. Dayan, X. Wang, M. Bikson, W. K. Doyle, O. Devinsky, and L. C. Parra, “Measurements and models of electric fields in the *in vivo* human brain during transcranial electric stimulation,” *eLife*, vol. 6, p. e18834, Feb. 2017.
- [11] J. P. Dmochowski, A. Datta, Y. Huang, J. D. Richardson, M. Bikson, J. Fridriksson, and L. C. Parra, “Targeted transcranial direct current stimulation for rehabilitation after stroke,” *NeuroImage*, vol. 75, pp. 12–19, Jul. 2013.
- [12] Y. Huang, C. Thomas, A. Datta, and L. C. Parra, “Optimized tDCS for Targeting Multiple Brain Regions: An Integrated Implementation,” in *2018 40th Annual International Conference of the IEEE Engineering in Medicine and Biology Society (EMBC)*, Jul. 2018, pp. 3545–3548.